

## Parity- and time-odd atomic multipoles in magnetoelectric $\text{GaFeO}_3$ as seen via soft x-ray Bragg diffraction

U. Staub,<sup>1</sup> Y. Bodenthin,<sup>1</sup> C. Piamonteze,<sup>1</sup> M. García-Fernández,<sup>1</sup> V. Scagnoli,<sup>2</sup> M. Garganourakis,<sup>1</sup> S. Koohpayeh,<sup>3</sup> D. Fort,<sup>3</sup> and S. W. Lovesey<sup>4,5</sup>

<sup>1</sup>Swiss Light Source, Paul Scherrer Institut, CH 5232 Villigen PSI, Switzerland

<sup>2</sup>European Synchrotron Radiation Facility, F 38043 Grenoble Cedex 9, France

<sup>3</sup>Department of Metallurgy and Materials, University of Birmingham, Birmingham B15 2TT, United Kingdom

<sup>4</sup>ISIS Facility, Harwell Science and Innovation Campus, Oxfordshire OX11 0QX, United Kingdom

<sup>5</sup>Diamond Light Source Ltd., Oxfordshire OX11 0DE, United Kingdom

(Received 15 September 2009; published 23 October 2009)

We present resonant soft x-ray Bragg diffraction data on the space-group forbidden (010) reflection at the Fe  $L_{2,3}$  edges of magnetoelectric  $\text{GaFeO}_3$ . Observed intensities give direct evidence for strange atomic multipoles that violate both time and space inversion, in particular a magnetoelectric quadrupole. The discovery of magnetoelectric multipoles in the open  $3d$  shell is a direct measure of coupling between magnetic and electric properties and a basis to a microscopic understanding of magnetically induced multiferroics.

DOI: 10.1103/PhysRevB.80.140410

PACS number(s): 75.80.+q, 75.25.+z, 75.50.Gg

Materials with coexistence of spontaneous order of electric polarization and magnetization, often called multiferroics, are of intense current interest,<sup>1–4</sup> because they may offer the opportunity to change magnetization by electric fields and vice versa. Our reported use of resonant x-ray Bragg diffraction to detect strange atomic multipoles hosted by such a complex material emulates atomic parity-violation experiments to measure the nuclear anapole<sup>5</sup> and it is the method of choice to detect strange multipoles predicted in advanced simulations of complex materials.<sup>6</sup>




A magnetic site in a multiferroic is not a center of inversion symmetry (or parity odd), and electron properties may be represented by atomic multipoles that violate both space and time inversion.<sup>7,8</sup> Such multipoles are labeled magnetoelectric and are directly related to the coupling between magnetism and electric polarization on the atomic level. They are caused by overlap of wave functions with different parity of the magnetic site with those of the neighboring ligands. Examples of simple geometrical representations of an anapole (or toroidal moment) are a solenoid formed into a torus, with an even number of windings, or four spin-bearing ions in the (001) plane of a tetragonal unit cell with a head-to-tail arrangement of the spins. The source for the toroidal moments is a time-odd axial vector  $\mathbf{\Omega}$  with components  $\mathbf{\Omega} \propto (\mathbf{E} \times \mathbf{H})$  in the same way as electric ( $\mathbf{E}$ ) and magnetic ( $\mathbf{M}$ ) fields are source vectors for polarization and magnetization, respectively. The relation between this anapole and multiferroic properties is of current interest.<sup>9</sup> Magnetic ions in multiferroics have nonzero expectation value for magnetoelectric multipoles, e.g.  $\mathbf{\Omega}$ . Magnitudes measure the wave function overlap responsible for the magnetoelectric coupling. It is this coupling, which causes the electric polarization in magnetically driven multiferroics.<sup>1,4</sup> Consequently, studies of atomic magnetoelectric multipole moments is an essential test ground for microscopic models describing magnetically driven multiferroics.

In a more basic view, atomic multipoles of an open valence shell can be separated in respect to inversion symmetry (parity), as shown in Table I. Parity-even atomic multipoles,

such as electric charge, magnetic dipoles or electric quadrupoles are broadly studied because they are detectable with many techniques, including by parity-even electric-electric dipole E1-E1 transitions. Parity odd atomic multipoles are similar fundamental entities, but are much less familiar due to the difficulty to directly observe them. The magnetoelectric quadrupole and monopole have so far not been unambiguously detected. Observation of magnetoelectric multipoles may arise from the E1-M1 (M1 magnetic dipole) event, which is parity odd.<sup>5,10,11</sup> Our study here completes the family of observed atomic magnetoelectric multipoles in solids, including magnetic charge (magnetoelectric monopole) and the magnetoelectric quadrupole. We show here how they contribute directly to the intensity of Bragg diffraction at resonance.

An ideal system for studying magnetoelectric multipoles is gallium ferrate ( $\text{GaFeO}_3$ ), known to be the first ferrimag-

TABLE I. (Color online) Parity odd atomic operators of different rank used to represent time-odd (magnetoelectric) and time-even (polar) multipoles are shown. For comparison, regular parity-even multipoles are included (“electric charge,” “magnetic moment,” and “orbital”). The basic operators are  $\mathbf{R}$  position,  $\boldsymbol{\mu}$  magnetic moment, and  $\mathbf{\Omega} = \boldsymbol{\mu} \times \mathbf{R} - \mathbf{R} \times \boldsymbol{\mu}$  anapole operator. Expectation values of the magnetoelectric and polar monopole operators (Ref. 12) are analogous to magnetic charge and chirality, or helicity. Useful cartoon representations accompany each tensor rank, and highlighted operators feature in the analysis of our data.

	Tensor rank K			Event
	0 	1 	2 	
Magneto-electric	$\boldsymbol{\mu} \cdot \mathbf{R}$	$\mathbf{\Omega}$	$\{\boldsymbol{\mu} \otimes \mathbf{R}\}^2$	E1-M1
Polar	$\mathbf{\Omega} \cdot \boldsymbol{\mu}$	$\mathbf{R}$	$\{\mathbf{\Omega} \otimes \boldsymbol{\mu}\}^2$	E1-M1
Parity-even	1	$\boldsymbol{\mu}$	$\{\boldsymbol{\mu} \otimes \boldsymbol{\mu}\}^2$	E1-E1

netic, piezoelectric studied material.<sup>13</sup> At room temperature the orthorhombic structure of gallium ferrate belongs to the  $C_{2v}$  polar crystal class,<sup>14,15</sup> with spontaneous electric polarization along the  $b$ -axis. Sites in this structure occupied by Fe ions ( $3d^5$ ) have no symmetry. Below  $T \approx 200$  K, collinear ferrimagnetism,<sup>16</sup> due to an admixture of the Ga and Fe sites, and the magnetoelectric effect<sup>17</sup> develop, with the magnetic easy axis along the crystal  $c$ -axis. The absence of site symmetry for magnetic iron is the necessary ingredient for existence of magnetoelectric multipoles. Results for gallium ferrate derived from dichroic signals, gathered in the optical<sup>18</sup> and x-ray<sup>19</sup> regions, and resonant x-ray Bragg diffraction at the iron  $K$ -edge (Ref. 20) appeared recently. These measurements are sensitive to magnetoelectric multipoles;<sup>10</sup> however, interpretation of Fe  $K$ -edge data are very complex due to the admixtures of higher rank multipole moments. Our resonant soft x-ray diffraction on space-group forbidden reflections give a *direct* measure of magnetoelectric multipoles at the iron site with  $3d$  character, as probed by the Fe  $L_{2,3}$  edges.

Stoichiometric amounts of  $Ga_2O_3$  (99.99% purity) and  $Fe_2O_3$  ( $\geq 99.0\%$  purity) were thoroughly ground together and then synthesized at 1200 °C for 20 h in air with an intermediate grinding after 10 h. The powder was then compacted into a rod and sintered in a vertical tube furnace at 1350 °C for 30 h in air. Single crystals were grown under 8.5 bar oxygen at zoning rate of 2 mm/h. A single crystal was cut along the (0 1 0) surface and glued on to the copper sample holder mounted in a He flow cryostat reaching temperatures between 10 and 300 K. Resonant soft x-ray diffraction experiments were performed on the RESOXS end-station<sup>21</sup> at the SIM beamline of the Swiss Light Source of the Paul Scherrer Institut, Switzerland. Experiments were performed using linear horizontal or vertical polarized light, leading to  $\pi$  or  $\sigma$  incident photon polarization in a horizontal scattering geometry, respectively. Polarization analysis of secondary radiation and azimuthal-angle scans were performed as in Refs. 21 and 22. The magnetization of the sample was changed by mounting a permanent magnet on the transfer system, leading to an effective field of 0.2 T on the sample. Experiments are performed in zero magnetic fields (remanence).

The inset of Fig. 1(a) shows rocking curves of the space-group forbidden (0 1 0) reflection at the iron  $L_3$  absorption edge, gathered in polarization channels  $\sigma'\sigma$  and  $\pi'\sigma$  at  $T = 100$  K, deep inside the ferrimagnetic phase ( $T < T_c \approx 200$  K). Intensities gathered in this phase [panels (a) and (b), Fig. 1] are independent of the state of primary polarization, which confirm the anticipated absence of scattering in channels  $\sigma'\sigma$  and  $\pi'\pi$  at all energies, and depend strongly on the azimuthal angle. Comparison of panels (a) and (b) with panel (c), Fig. 1, shows that the onset of magnetic order, at  $T_c$ , generates signal enhancement. The correlation between intensity and magnetic order is amplified by our observation of intensity as a function of temperature at the  $L_3$  edge (Fig. 2). Already seen in the energy dependence [Fig. 1(c)], above  $T_c$ , this intensity is constant and nonzero, and relatively weak. Below  $T_c$  intensity strongly increases, with similar temperature behavior to the magnetization. Because the (0 1 0) reflection is forbidden by the established chemical

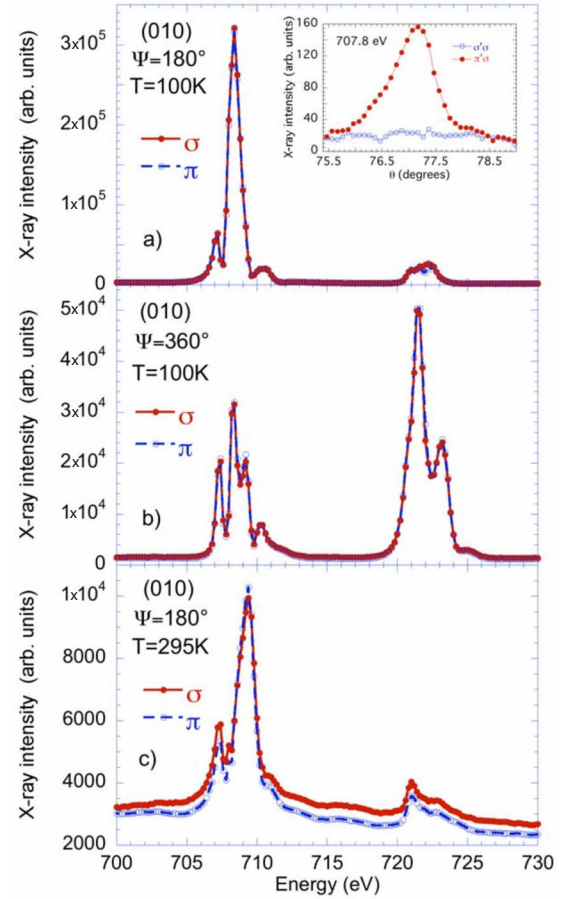


FIG. 1. (Color online) Energy dependence of the (0 1 0) Bragg reflection with different azimuthal angles ( $\psi$ ), temperatures ( $T$ ) and primary polarizations,  $\sigma$  and  $\pi$ . Inset to panel (a) are rocking curves taken at 100 K,  $\psi = 150^\circ$ , and energy = 708.4 eV ( $L_3$  edge) with fixed outgoing polarization  $\sigma$ .

and magnetic structures, additional intensity occurring below  $T_c$  cannot be caused by the usual electric dipole transition E1-E1. Rather, this additional intensity is a *direct* measure of time and parity-odd multipoles absent in the paramagnetic phase,  $T > T_c$ .

For a model to be credible to describe these data it must comply with two conditions. First, it must incorporate the

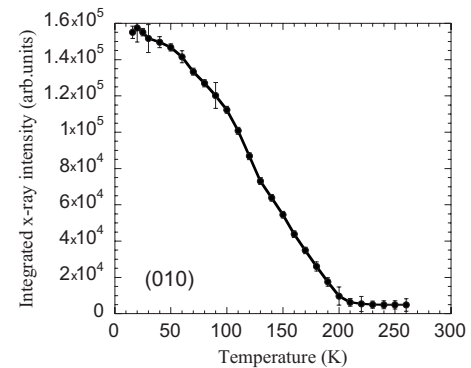


FIG. 2. Temperature dependence of the (0 1 0) reflection intensity at the  $L_3$  edge.

established crystal and magnetic structures of gallium ferrate. Second, the model must respect all symmetries embedded in photon scattering amplitudes derived from quantum electrodynamics, with enhancement by E1, and M1 (and E2, electric quadrupole) resonant events.<sup>11,23</sup>

These requirements are met by our model which has already proved its worth by successfully describing existing diffraction data, gathered at the iron *K* edge.<sup>10</sup> Evaluated for space-group forbidden reflections of the type (0 *k* 0) with odd *k*, the structure factors result for the rotated light channels in as a sum of three components<sup>10,12</sup>

$$F^{E1-E1} = 4A \cos \theta \cos \psi \langle T_1^2 \rangle'', \quad (1)$$

$$F^{E1-M1} = -i2\sqrt{2}B \sin 2\theta \cos \psi \langle U_0^1 \rangle, \quad (2)$$

$$F^{E1-M1} = -A/\sqrt{3} \{ 8 \sin^2 \theta \langle G_0^0 \rangle + \sqrt{2} [2 + \cos^2 \theta (1 + 3 \cos 2\psi)] \times \langle G_0^2 \rangle + 2\sqrt{3} [2 + \cos^2 \theta (1 - \cos 2\psi)] \langle G_2^2 \rangle' \}. \quad (3)$$

Here, *A* and *B* are complex factors that are fully determined by the model and not free to fit, and  $\theta$  is the Bragg angle. There are five purely real atomic multipoles:  $\langle T_1^2 \rangle''$  is the imaginary part of the familiar parity-even quadrupole from the E1-E1 event, often called Templeton and Templeton scattering,<sup>24</sup>  $\langle U_0^1 \rangle$  is the polar dipole,  $\langle G_0^2 \rangle$  and  $\langle G_2^2 \rangle'$  are components of the magnetoelectric quadrupole and, lastly,  $\langle G_0^0 \rangle$  is magnetic charge (magnetoelectric monopole). The model predicts that the diffraction amplitude is zero in polarization channels with identical primary and secondary states ( $\sigma'\sigma$  and  $\pi'\pi$ ) and shows that  $I_{\pi\sigma}(E) = I_{\sigma\pi}(E)$  in agreement with Figs. 1 and 3. The model shows contribution from the iron magnetoelectric multipoles [Eq. (3)] listed in Table I but not the magnetic dipole.

Confidence in assignment of the additional intensity in the ferrimagnetic state, to magnetoelectric multipoles is bolstered by observation of its dependence on applied magnetic fields. First, intensity tracks the polarity (+−) of an applied field (0.2 T) along the magnetic easy *c* axis [Fig. 3(a)]. Second, rotation by 180° of the crystal around *b* (azimuth) normal to the easy axis is equivalent to reversing the polarity of the field along this axis [Fig. 3(b)].

For an analysis of our measurements, consider what is expected with resonant diffraction by ferric ions (Fe<sup>3+</sup>). The atomic structure,  $3d^5$ , is spherically symmetric with a magnetic moment exclusively due to five parallel spins (*S*-state ion). For the corresponding E1-E1 event, the only source of diffraction is the magnetic moment, which is zero in the paramagnetic state and invisible in the ordered, ferrimagnetic state, because magnetization parallel to the crystal *c* axis does not contribute to diffraction at (0 1 0). Furthermore, all parity-odd multipoles are identically zero for an isolated *S*-state ion so the E1-M1 event makes no contribution to scattering. Hence, our observation of intensity at (0 1 0) from a paramagnetic crystal [Fig. 1(c)] records contamination of the ferric state,  $3d^5$ . The noncentrosymmetric crystal-field, configuration interaction, and covalent bonding with neighboring ligand ions are potential candidate mechanisms for departures from an *S*-state. These same mechanisms mix  $3d$  orbitals at iron sites with other orbitals, including orbitals

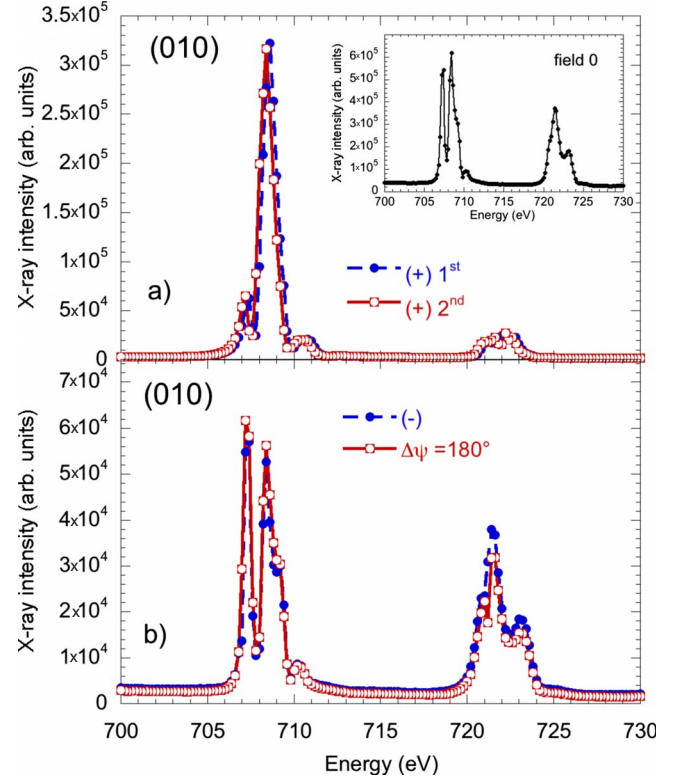


FIG. 3. (Color online) Magnetic field dependence of the (0 1 0) reflection at  $\psi = 150^\circ$ ,  $T = 100$  K, and  $\sigma$  primary polarization. Intensities in panel (a) have (+) polarity, panel (b) has (−) polarity or are collected in (+) polarity but  $\psi$  differs by 180° from the angle used in the other three sets of data. Open circles in panel (a) are obtained following recovery of the magnetic state from (−) in (b) panel. Inset to panel (a) is data collected prior to the imposition of a magnetic field on the sample.

with a different parity. Such admixed orbitals allow parity-odd multipoles in the intensity to occur in the E1-M1 event.

Intensities as a function of azimuthal angle, displayed in Fig. 4, are adequately described by the expression  $I_0 = |t + \alpha \cos(\psi) + \beta \cos(2\psi)|^2$ , derived from Eqs. (1)–(3), which is shown in the figure by a continuous curve. In consequence, quantities *t*,  $\alpha$  and  $\beta$  are atomic multipoles that describe ground-state properties of Fe valence electrons. A monopole (charge) cannot cause intensity to depend on the azimuthal angle, of course, and thus it is part of *t* only. One finds that *t* and  $\beta$  are purely real, while  $\alpha$  is complex with a phase fully determined by the model. Moreover, *t* and  $\beta$  are composed of magnetoelectric multipoles, which vanish in the paramagnetic state, while  $\alpha$  is composed of time-even multipoles.

Inspection of Fig. 4 shows that, *t* and  $\beta$  are different from zero at both *L*-edges and, therefore, our azimuthal-angle scans are further evidence that intensities are directly related to magnetoelectric multipoles. Fitting our data at the *L*<sub>3</sub> edge to  $I_0$  reveals the parity-even quadrupole and polar dipole contribute in a not well defined ratio  $\approx 1:0.5$ . Magnitudes of parity-even and magnetoelectric quadrupoles are in a ratio  $\approx 1:2.4$ , while magnetic charge is ambiguous in the fit to data, with error in excess of a relatively small inferred value.



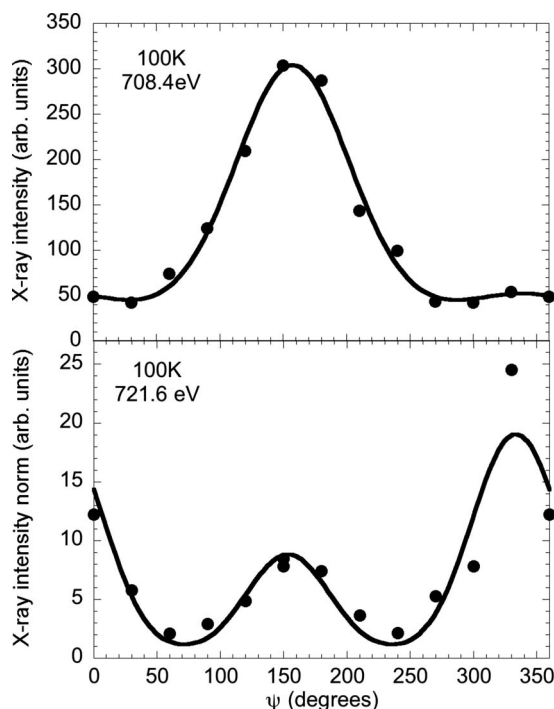


FIG. 4. Azimuthal angle dependence of the (0 1 0) reflection at  $T=100$  K. Intensities are collected at the  $L_2$  and  $L_3$  edges using  $\sigma$  primary polarization. Continuous curves are fits to data explained in the text.

Observation of intensity in the paramagnetic state, with a  $\{\cos(\psi)\}^2$ -like dependence on the azimuthal angle (not shown), proves that the ferric ion is not  $S$ -like and iron va-

lence electrons possess an orbital contribution. Analysis of previous  $K$ -edge experiments demonstrated the role of the E1-M1.<sup>10</sup> A possible relevance of the E1-E2 event at the Fe  $L_{2,3}$  edges engages an admixture of  $3d$  and delocalized higher energetic  $4f$  states. Such would mean that the E1-E1 and E1-E2 resonant events are at significantly different energies, which is not consistent with our experiment. Therefore, a coherent sum of E1-E1 and E1-M1 resonant events is responsible for the Bragg intensities we observe. Because of the absence of a magnetic-dipole signal, the observed intensities represent the direct observation of magnetoelectric multipoles, independent of the event used in the interpretation of data.

In conclusion, the discovery of a magnetoelectric quadrupole by resonant Bragg diffraction in  $\text{GaFeO}_3$  is a manifestation of exactly those electrons that deliver the magnetoelectric effect. Measured energy profiles pose an interest for electronic calculations directly testing the relevant hybridization between oxygen and Fe  $3d$  wave functions of opposite parity, creating the magnetoelectric interaction. Observation of magnetoelectric multipoles through space-group forbidden reflections indicate their antiferro type of order. The *direct* observation of atomic like magnetoelectric multipoles is of immense importance for microscopic models describing the magnetic and electronic properties of magnetically driven multiferroics as they may represent the electronic order-parameter.

We thank K. S. Knight for many valuable discussions and E. M. Duke for a critical reading of the Rapid Communication. We acknowledge financial support by the Swiss National Science Foundation.

- <sup>1</sup>S. W. Cheong and M. Mostovoy, *Nature Mater.* **6**, 13 (2007).
- <sup>2</sup>T. Kimura, T. Goto, H. Shintani, K. Ishizaka, T. Arima, and Y. Tokura, *Nature (London)* **426**, 55 (2003).
- <sup>3</sup>W. Eerenstein, N. D. Mathur, and J. F. Scott, *Nature (London)* **442**, 759 (2006).
- <sup>4</sup>M. Fiebig, *J. Phys. D* **38**, R123 (2005).
- <sup>5</sup>K. Tsigutkin *et al.*, *Phys. Rev. Lett.* **103**, 071601 (2009).
- <sup>6</sup>F. Cricchio *et al.*, *Phys. Rev. Lett.* **103**, 107202 (2009).
- <sup>7</sup>P. Carra and R. Benoist, *Phys. Rev. B* **62**, R7703 (2000).
- <sup>8</sup>H. Schmid, *Ferroelectrics* **252**, 41 (2001).
- <sup>9</sup>D. Khomskii, *Physics* **2**, 20 (2009).
- <sup>10</sup>S. W. Lovesey, K. S. Knight, and E. Balcar, *J. Phys.: Condens. Matter* **19**, 376205 (2007).
- <sup>11</sup>S. P. Collins, S. W. Lovesey, and E. Balcar, *J. Phys.: Condens. Matter* **19**, 213201 (2007).
- <sup>12</sup>S. W. Lovesey and V. Scagnoli, *J. Phys. Condens. Matter* (to be published).
- <sup>13</sup>J. P. Remeika, *J. Appl. Phys.* **31**, S263 (1960).
- <sup>14</sup>T. Arima, D. Higashiyama, Y. Kaneko, J. P. He, T. Goto, S. Miyasaka, T. Kimura, K. Oikawa, T. Kamiyama, R. Kumai, and Y. Tokura, *Phys. Rev. B* **70**, 064426 (2004).
- <sup>15</sup>E. A. Wood, *Acta Crystallogr.* **13**, 682 (1960).
- <sup>16</sup>R. B. Frankel, N. A. Blume, S. Foner, A. J. Freeman, and M. Schieber, *Phys. Rev. Lett.* **15**, 958 (1965).
- <sup>17</sup>G. T. Rado, *Phys. Rev. Lett.* **13**, 335 (1964).
- <sup>18</sup>J. H. Jung, M. Matsubara, T. Arima, J. P. He, Y. Kaneko, and Y. Tokura, *Phys. Rev. Lett.* **93**, 037403 (2004).
- <sup>19</sup>M. Kubota, T. Arima, Y. Kaneko, J. P. He, X. Z. Yu, and Y. Tokura, *Phys. Rev. Lett.* **92**, 137401 (2004).
- <sup>20</sup>T. Arima, J. H. Jung, M. Matsubara, M. Kubota, J. P. He, Y. Kaneko, and Y. Tokura, *J. Phys. Soc. Jpn.* **74**, 1419 (2005).
- <sup>21</sup>U. Staub, V. Scagnoli, Y. Bodenthin, M. García-Fernández, R. Wetter, A. M. Mulders, H. Grimmer, and M. Horisberger, *J. Synchrotron Radiat.* **15**, 469 (2008).
- <sup>22</sup>U. Staub, V. Scagnoli, A. M. Mulders, K. Katsumata, Z. Honda, H. Grimmer, M. Horisberger, and J. M. Tonnerre, *Phys. Rev. B* **71**, 214421 (2005).
- <sup>23</sup>S. W. Lovesey, E. Balcar, K. S. Knight, and J. Fernandez-Rodriguez, *Phys. Rep.* **411**, 233 (2005).
- <sup>24</sup>D. H. Templeton and L. K. Templeton, *Acta Crystallogr., Sect. A: Cryst. Phys., Diff., Theor. Gen. Crystallogr.* **38**, 62 (1982).